

Vertex models for the product of a permuted-basement Demazure atom and a Schur polynomial

Timothy C. Miller

Department of Combinatorics and Optimization
 University of Waterloo
 Waterloo, ON N2L 3G1
 Canada

tcmiller@uwaterloo.ca

March 13, 2025

Abstract

We give the first positive combinatorial rule for expanding the product of a permuted-basement Demazure atom and a Schur polynomial. Special cases of permuted-basement Demazure atoms include Demazure atoms and characters. These cases have known tableau formulas for their expansions when multiplied by a Schur polynomial, due to Haglund, Luoto, Mason and van Willigenburg. We find a vertex model formula, giving a new rule even in these special cases, extending a technique introduced by Zinn-Justin for calculating Littlewood–Richardson coefficients.

We derive a coloured vertex model for permuted-basement Demazure atoms, inspired by Borodin and Wheeler’s model for non-symmetric Macdonald polynomials. We make this model compatible with an uncoloured vertex model for Schur polynomials, putting them in a single framework. While previous work on structure coefficients via vertex models relies on solutions to the Yang–Baxter equation, a remarkable feature of our construction is that the Yang–Baxter equation does not hold; we derive a weaker analogue that is sufficient to show our result.

1 Introduction

The *Schur polynomials* $s_\lambda(x)$, indexed by partitions λ , are an important \mathbb{Z} -basis for the ring of symmetric polynomials. The product of two Schur polynomials expands into a linear

combination with positive integer structure coefficients, called *Littlewood–Richardson coefficients*. These integers have many important applications, particularly in the representation theory of the general linear group and symmetric group, Schubert calculus and algebraic combinatorics. There are many combinatorial rules for computing these integers, the original being the eponymous Littlewood–Richardson rule [24].

Knutson, Tao and Woodward developed an alternative formula for Littlewood–Richardson coefficients, calculated as the number of certain tilings called *puzzles* [18, 19]. Puzzles were brought into the context of integrable systems by Zinn-Justin who reproved this rule, envisioning a particle model which places puzzles and Schur polynomials in one unified picture [33]. We build on this technique, giving the first combinatorial formula for the product of a Schur polynomial with a *permuted-basement Demazure atom* $\mathcal{A}_\alpha^\sigma(x)$, indexed by weak compositions α with permutation parameter σ .

We derive a manifestly positive, combinatorial rule for the structure coefficients $a_{\alpha\lambda}^\beta(\sigma)$ in the expansion

$$\mathcal{A}_\alpha^\sigma(x)s_\lambda(x) = \sum_{\beta} a_{\alpha\lambda}^\beta(\sigma)\mathcal{A}_\beta^\sigma(x),$$

where the summation is over weak compositions β .

Several bases of the ring of multivariate polynomials are known to expand positively when multiplied by a Schur polynomial [30]. Two well-known bases that exhibit this phenomenon are *Demazure atoms* and *Demazure characters*. Demazure characters, also called key polynomials, were introduced in [14] and studied combinatorially in [23]. They are characters of representations of a Borel subgroup, known as Demazure modules, and they generalize Schur polynomials. Demazure characters are also a special case of Kohnert polynomials [3]. Haglund, Luoto, Mason and van Willigenburg give positive rules for the products of a Schur polynomial with a Demazure atom or character, expressed in terms of certain tableaux known as skyline fillings [17]. There are many interesting open problems regarding expansions of Demazure polynomials, such as whether the product of two characters expands positively into atoms [29].

The polynomials $\mathcal{A}_\alpha^\sigma(x)$ are a specialization of *permuted-basement non-symmetric Macdonald polynomials* $E_\alpha^\sigma(x; q, t)$, introduced by Ferreira in [15] and expanded on by Alexandersson in [2]. We follow the conventions of Alexandersson, setting $\mathcal{A}_\alpha^\sigma(x) := E_\alpha^\sigma(x; 0, 0)$; note that some conventions in the literature reverse the order of α . The author’s work in a FPSAC extended abstract for this paper [26] originally considered separate models for Demazure atoms and characters. Now both are captured by one model depending on the parameter σ where $\sigma = (1, \dots, n)$ is the atom case and $\sigma = (n, \dots, 1)$ is the character case.

Vertex models are mathematical frameworks in statistical mechanics used to study particle systems. A notable example is the six-vertex or square-ice model; see [4] for detailed discussion. Each configuration of vertices in a graph is assigned a weight contributing to its *partition function*. Vertex models are often in a two-dimensional lattice where vertices may be represented by tiles, which is the convention we adopt in this paper.

Vertex model approaches have shown increasing promise in Schubert calculus and algebraic combinatorics with many recent papers demonstrating their applicability, e.g. [1, 5, 6, 9, 12, 13, 16, 20, 21, 22, 27, 31]. Often, an important polynomial can be realized as the partition function of a vertex model, making analysis amenable to a standard set of techniques from integrable systems. Schur polynomials, Demazure atoms and non-symmetric Macdonald polynomials all have vertex model formulations. Our model for $\mathcal{A}_\alpha^\sigma(x)$ is inspired by Borodin and Wheeler’s model for $E_\alpha^\sigma(x; q, t)$ [7], but we make significant modifications. Our model bears more resemblance to the model for Demazure atoms given by Brubaker, Buciumas, Bump and Gustafsson [8]; see Remark 2.3.

Our proof is completely combinatorial. We establish equivalence by gluing vertex models together in two different ways, similar to [32, 33]. Unlike previous results, which rely on solving the *Yang–Baxter equation*, we use a weaker analogue stated in Lemma 6.3. Our equation only works for certain boundary conditions, which happily hold in this case. Buciumas and Scrimshaw [10] have vertex models for Sp_{2n} and SO_{2n+1} Demazure atoms and characters which also do not satisfy a Yang–Baxter equation, which they term quasi-solvable.

Our results suggest further applications, such as extensions to the Grothendieck models in [32]. *Grothendieck polynomials*, *Lascoux atoms* and *Lascoux polynomials* are the K -theoretic analogues of Schur polynomials, Demazure atoms and Demazure characters respectively. Orelowitz and Yu have recently given a tableau formula for the expansion of a Lascoux polynomial and a stable Grothendieck [28]. Vertex models for Lascoux polynomials and atoms are also given by Buciumas, Scrimshaw and Weber [11].

A benefit of this approach is that we may develop vertex models independently and then fit into this framework, allowing one to test rules assuming a Yang–Baxter equation or an analogue such as Lemma 6.3 holds. As an offshoot, our notion of *σ -extendable*, given in Section 3, gives rise to a poset on weak compositions for each σ , which can be the subject of future work.

In Section 2, we introduce a vertex model for Schur polynomials and our model for permuted-basement Demazure atoms. Section 3 gives the skyline formulation for permuted-basement Demazure atoms and introduces the σ -extendable relation, which allows a recursive decomposition of these polynomials in Theorem 3.4. In Section 4, we show that our

vertex models also satisfy this recurrence, making a bijection clear. In Section 5, we state our expansion rule, Theorem 5.2, and then prove it in Section 6. We reserve proof of our key technical result, the Column Lemma 6.3, for Section 7.

2 Vertex models for permuted-basement Demazure atoms and Schur polynomials

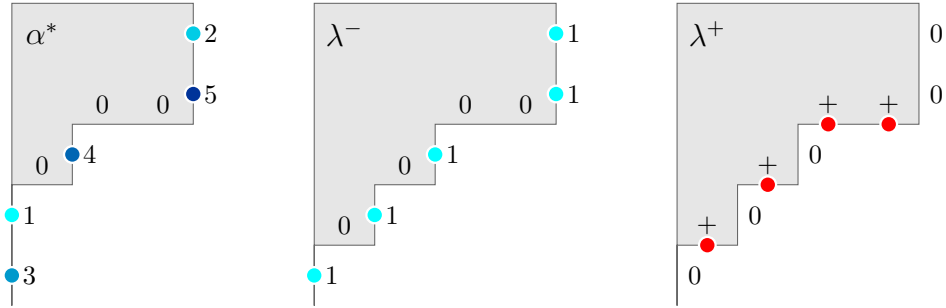
We give vertex model formulations for permuted-basement Demazure atoms and Schur polynomials, using the convention of depicting “vertices” in the models with tiles, aligning with [32, 33].

Throughout, $x = (x_1, \dots, x_n)$ is a list of n variables and we set $[n] := \{1, \dots, n\}$. A **weak composition** $\alpha = (\alpha_1, \dots, \alpha_n)$ is a sequence of non-negative integers. Each integer α_i is the **part** of α at index i and the **length** of α is its number of parts, denoted $\text{len}(\alpha)$. The largest part in α is denoted $\max(\alpha)$. A **partition** $\lambda = (\lambda_1, \dots, \lambda_n)$ is a weak composition with parts sorted in descending order. A **permutation** $\sigma = (\sigma(1), \dots, \sigma(n))$ is an ordering of the integers in $[n]$. Throughout, α and β are weak compositions, λ is a partition, σ is a permutation and all have length n .

We label boundaries in our models with strings that re-encode α or λ . Let $\mu = \text{sort}(\alpha)$ be the partition with the same parts as α sorted in descending order. Enclose the Young diagram of μ (in English convention) within the top left corner of a rectangle with a northeast lattice path as depicted in Example 2.1. Label east steps 0. Label north steps in vertical v (after v east steps) with the indices i of all parts satisfying $\alpha_i = v$, sorted in descending order moving north. We obtain the string α^* by reading labels along the lattice path from southwest to northeast.

We re-encode a partition λ similarly in two ways, with strings λ^- and λ^+ . For λ^- , label east steps 0 and north steps 1. For λ^+ , label east steps with the symbol $+$ and label north steps 0. Read strings from the lattice path as before. The string λ^+ appears in later sections.

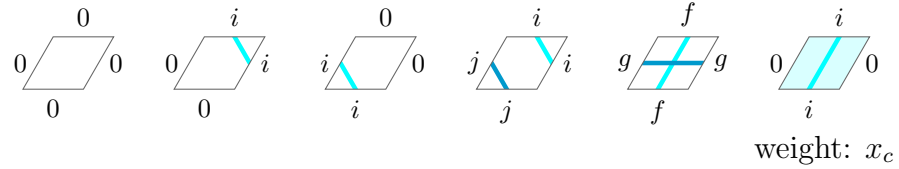
Example 2.1. We depict our labelling procedure for $\alpha = (0, 3, 0, 1, 3)$ and $\lambda = (4, 4, 2, 1, 0)$.



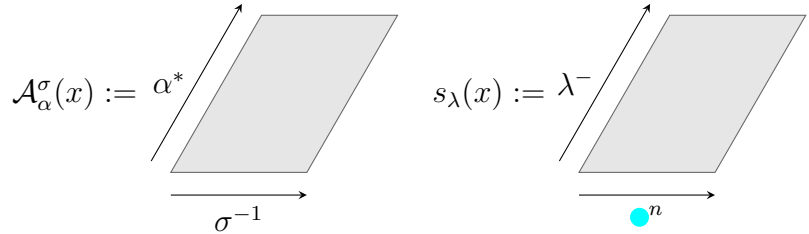
Reading the labels from southwest to northeast produces the desired strings.

$$\begin{aligned} \alpha^* &= 31040052 \\ \lambda^- &= 101010011 \\ \lambda^+ &= 0+0+0++00 \end{aligned}$$

We construct our models by filling a lattice with rhombic tiles, depicted below, where i, j, f, g are in $[n]$, $i \leq j$, and $\sigma(f) < \sigma(g)$.

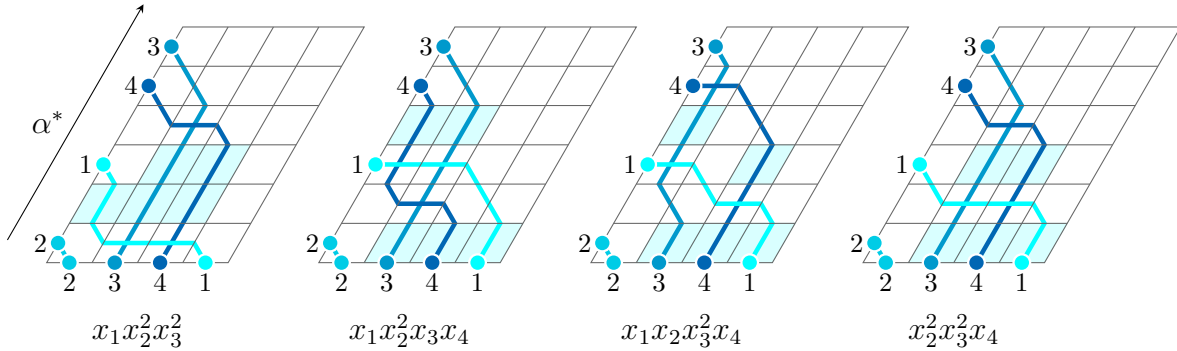


The final tile has weight x_c , where c is the column number that the tile occurs in, and all other tiles have weight 1. Columns are numbered 1 to n from left to right. We say tiles of weight 1 are *trivial* and the final tile is *nontrivial*. We define *permuted-basement Demazure atoms (atoms)* $\mathcal{A}_\alpha^\sigma(x)$ and *Schur polynomials* $s_\lambda(x)$ in terms of the partition function of vertex models with these tiles. We place the tiles within a rhombic lattice with fixed boundary labels. Labels on edges between tiles or a tile and the boundary must match. We schematically outline both models below:

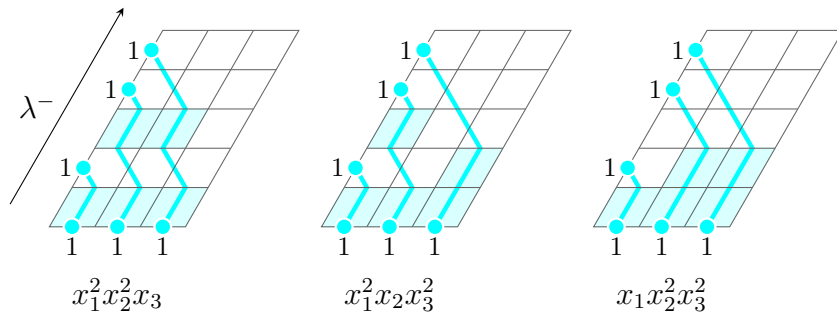


We call the model for $\mathcal{A}_\alpha^\sigma(x)$ the *atom model* and the model for $s_\lambda(x)$ the *Schur model*. Label the left boundary of the atom model with α^* and the bottom with σ^{-1} (this choice makes our polynomials align with the definition in terms of skyline fillings in Section 3). Label the left boundary of the Schur model with λ^- and the bottom with all 1's, denoted by \bullet^n . Label unspecified boundaries with all 0's. We refer to a legal tiling of a model as a *filling*. A filling's weight is the product of its tile weights and the sum of all filling weights is called the *partition function* of the model.

Example 2.2. Let $\alpha = (1, 0, 2, 2)$ and $\sigma = 4123$, so that $\sigma^{-1} = 2341$ and $\alpha^* = 201043$. There are four fillings of the atom model, showing $\mathcal{A}_\alpha^\sigma(x_1, x_2, x_3, x_4) = x_1x_2^2x_3^2 + x_1x_2^2x_3x_4 + x_1x_2x_3^2x_4 + x_2^2x_3^2x_4$.



Next, let $\lambda = (2, 2, 1)$, so that $\lambda^- = 01011$. There are three fillings of the Schur model, showing $s_\lambda(x_1, x_2, x_3) = x_1^2x_2^2x_3 + x_1^2x_2x_3^2 + x_1x_2^2x_3^2$.



Remark 2.3. The Schur model is the same as the one considered by Zinn-Justin in [33] and we can think of the atom model as a “coloured” version of the Schur model. Brubaker, Buciumas, Bump and Gustafsson [8] have a vertex model for Demazure atoms, which is the case where $\sigma = \text{id}$. Our tiles are essentially the same as their vertices in this case, with

a permutation applied to the colours. Their model also has different weights, picking up an extra factor x^ρ .

3 Skyline fillings and σ -extendable decompositions

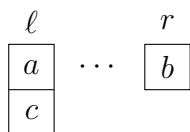
We give an alternative definition of atoms in terms of the semi-skyline augmented fillings of [25] and use this definition to give a recursive decomposition of atoms. A *semi-skyline augmented filling (SSAF)* of *shape* α with *basement* σ is a function

$$F : \{(i, j) \mid 0 \leq j \leq \alpha_i, i \in [n]\} \rightarrow \mathbb{Z}_+,$$

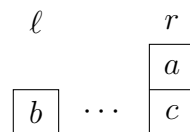
which must satisfy certain conditions. We refer to the pairs (i, j) in the domain of F as *cells* and write $F((i, j)) := F(i, j)$ as a shorthand. We say a cell is in F if it is in the domain of F . The *entry* of a cell c is the value $F(c)$ and a cell with entry e is an *e-cell* of F . The *basement* of a filling refers to cells $(i, 0)$ for $i \in [n]$, which are always assigned the entry $\sigma(i)$. SSAFs must have no *descents*, meaning $F(i, j + 1) \leq F(i, j)$ for $j \geq 0$.

Lastly, SSAFs must satisfy certain conditions for “triples,” which come in two flavours. Let $1 \leq \ell < r \leq n$; if $\alpha_\ell \geq \alpha_r$, a *type A triple* within columns ℓ and r is of the form $(\ell, i + 1), (r, i + 1), (\ell, i)$ for $i \geq 0$. If $\alpha_\ell < \alpha_r$, a *type B triple* within columns ℓ and r is of the form $(r, i + 1), (\ell, i), (r, i)$ for $i \geq 0$. We illustrate below, labelling cells with their entries a, b, c :

Type A:



Type B:



In either case, a triple is called *inversion* if $b \notin [a, c]$ and *coinversion* if $b \in [a, c]$. All triples within an SSAF are inversion. Denote the set of all SSAFs of α with basement σ by $\text{SSAF}_\sigma(\alpha)$. The polynomials $\mathcal{A}_\alpha^\sigma(x)$ are then given by a summation over fillings in $\text{SSAF}_\sigma(\alpha)$:

$$\mathcal{A}_\alpha^\sigma(x) = \sum_{F \in \text{SSAF}_\sigma(\alpha)} x^F,$$

where x^F is the product of $x_{F(c)}$ over all cells c in F .

Example 3.1. If $\alpha = (1, 0, 2, 1)$ and $\sigma = (2, 1, 4, 3)$, there are five fillings in $\text{SSAF}_\sigma(\alpha)$:

1		2		4	3
2	1	4	3		

1		3		4	3
2	1	4	3		

1		4		4	3
2	1	4	3		

2		3		4	3
2	1	4	3		

2		4		4	3
2	1	4	3		

This shows that $\mathcal{A}_\alpha^\sigma(x) = x_1x_2x_3x_4 + x_1x_3^2x_4 + x_1x_3x_4^2 + x_2x_3^2x_4 + x_2x_3x_4^2$.

Definition 3.2. Given weak compositions α and β of length n and $\sigma \in S_n$, we say that β is σ -*extendable* to α if $\alpha_i \geq \beta_i$ for $i \in [n]$ and the following conditions hold for each pair (ℓ, r) satisfying $1 \leq \ell < r \leq n$:

1. If $\alpha_\ell \geq \alpha_r$ and $\beta_\ell \geq \beta_r$, then $\alpha_r \leq \beta_\ell$.
2. If $\alpha_\ell < \alpha_r$ and $\beta_\ell < \beta_r$, then $\alpha_\ell < \beta_r$.
3. If $\alpha_\ell \geq \alpha_r$ and $\beta_\ell < \beta_r$, then $\alpha_r = \beta_r$ and $\sigma(\ell) < \sigma(r)$.
4. If $\alpha_\ell < \alpha_r$ and $\beta_\ell \geq \beta_r$, then $\alpha_\ell = \beta_\ell$ and $\sigma(\ell) > \sigma(r)$.

Lemma 3.3. Let $F \in \text{SSAF}_\sigma(\alpha)$ for a weak composition α of length n and $\sigma \in S_n$ and let $1 \leq \ell < r \leq n$.

1. If $\alpha_\ell \geq \alpha_r$ and $0 \leq a \leq \alpha_r$, then:
 - (a) If $F(\ell, a) < F(r, a)$, then $F(\ell, i) < F(r, i + 1)$ for all $0 \leq i \leq a - 1$.
 - (b) If $F(\ell, a) > F(r, a)$, then $F(\ell, i) > F(r, i)$ for all $a \leq i \leq \alpha_r$.
2. If $\alpha_\ell < \alpha_r$ and $0 \leq a \leq \alpha_\ell$, then:
 - (a) If $F(\ell, a) < F(r, a)$, then $F(\ell, i) < F(r, i + 1)$ for all $a \leq i \leq \alpha_\ell$.
 - (b) If $F(\ell, a) > F(r, a)$, then $F(\ell, i) > F(r, i)$ for all $0 \leq i \leq a$.

Proof. 1. Assume $\alpha_\ell \geq \alpha_r$ and $0 \leq a \leq \alpha_r$.

- (a) Suppose $F(\ell, a) < F(r, a)$. If $a = 0$, the inequality is vacuously satisfied. Otherwise, if $F(\ell, a - 1) \geq F(r, a)$, then $(\ell, a), (r, a), (\ell, a - 1)$ is a type A coinversion triple, so $F(\ell, a - 1) < F(r, a)$. Then by the descent condition, $F(\ell, a - 1) < F(r, a - 1)$ and by induction, we have $F(\ell, i) < F(r, i + 1)$ for all $0 \leq i \leq a - 1$.

(b) Suppose $F(\ell, a) > F(r, a)$. If $a = \alpha_r$, we are done. Otherwise, if $F(\ell, a + 1) \leq F(r, a + 1)$, then $(\ell, a + 1), (r, a + 1), (\ell, a)$ is a type A coinversion triple, so $F(\ell, a + 1) > F(r, a + 1)$. By induction, we have $F(\ell, i) > F(r, i)$ for all $a \leq i \leq \alpha_r$.

2. Assume $\alpha_\ell < \alpha_r$ and $0 \leq a \leq \alpha_\ell$.

(a) Suppose $F(\ell, a) < F(r, a)$. If $F(\ell, a) \geq F(r, a + 1)$ then $(r, a + 1), (\ell, a), (r, a)$ is a type B coinversion triple, so $F(\ell, a) < F(r, a + 1)$. If $a = \alpha_\ell$, we are done; otherwise, $F(\ell, a + 1) < F(r, a + 1)$ by the descent condition and by induction, we have $F(\ell, i) < F(r, i + 1)$ for all $a \leq i \leq \alpha_\ell$.

(b) Suppose $F(\ell, a) > F(r, a)$. If $a = 0$, we are done; otherwise, $F(\ell, a - 1) \geq F(\ell, a) > F(r, a)$ and thus $F(\ell, a - 1) > F(r, a - 1)$ since otherwise $(r, a), (\ell, a - 1), (r, a - 1)$ is a type B coinversion triple. By induction, we have $F(\ell, i) > F(r, i)$ for all $0 \leq i \leq a$.

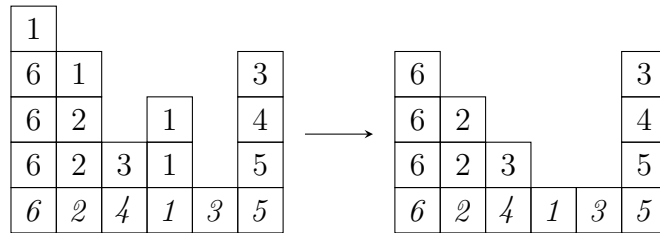
□

We prove that the atoms $\mathcal{A}_\alpha^\sigma(x)$ decompose into a summation over compositions β that are σ -extendable to α . Each such β is the shape of an SSAF that remains after deleting the non-basement 1-cells from a filling in $\text{SSAF}_\sigma(\alpha)$.

Theorem 3.4. *For a weak composition α of length n and $\sigma \in S_n$, we have*

$$\mathcal{A}_\alpha^\sigma(x) = \sum_{\beta \text{ } \sigma\text{-extendable to } \alpha} x_1^{|\alpha| - |\beta|} \mathcal{A}_\beta^\sigma(0, x_2, \dots, x_n).$$

Proof. For any filling $F \in \text{SSAF}_\sigma(\alpha)$, we produce a new filling F' obtained by deleting all 1-cells other than the basement. This yields a new filling on a weak composition β with the same basement as in the following example:



We first show that every such β is σ -extendable to α and that F' is in $\text{SSAF}_\sigma(\beta)$. It is clear that $\alpha_i \geq \beta_i$ for all $i \in [n]$, so we need to check the remaining conditions of Definition 3.2 for each pair of columns and verify that the relevant triples are inversion; let $1 \leq \ell < r \leq n$.

1. Assume $\alpha_\ell \geq \alpha_r$ and $\beta_\ell \geq \beta_r$. If $\alpha_r > \beta_\ell$, then cells $(\ell, \beta_\ell + 1)$ and $(r, \beta_\ell + 1)$ both exist in F and have entry 1, yielding a type A coinversion triple in F , so we have $\alpha_r \leq \beta_\ell$. All type A triples within columns ℓ and r in F' are inversion by assumption.
2. Assume $\alpha_\ell < \alpha_r$ and $\beta_\ell < \beta_r$. If $\alpha_\ell \geq \beta_r$, then cells (ℓ, β_r) and $(r, \beta_r + 1)$ both exist in F and have entry 1, yielding a type B coinversion triple in F , so we have $\alpha_\ell < \beta_r$. All type B triples within columns ℓ and r in F' are inversion by assumption.
3. Assume $\alpha_\ell \geq \alpha_r$ and $\beta_\ell < \beta_r$. If $\alpha_r > \beta_r$, then cells $(\ell, \beta_r + 1)$ and $(r, \beta_r + 1)$ both exist in F and have entry 1, yielding a type A coinversion triple in F , so we have $\alpha_r = \beta_r$. It is also true that the cell (ℓ, β_r) exists in F and has entry 1, so $F(\ell, \beta_r) < F(r, \beta_r)$ and, by case 1a of Lemma 3.3, we have $F(\ell, i) < F(r, i + 1) \leq F(r, i)$ for all $0 \leq i \leq \beta_r - 1$, which implies $\sigma(\ell) < \sigma(r)$ and also that all type B triples within columns ℓ and r in F' are inversion.
4. Assume $\alpha_\ell < \alpha_r$ and $\beta_\ell \geq \beta_r$. If $\alpha_\ell > \beta_\ell$, then cells $(\ell, \beta_\ell + 1)$ and $(r, \beta_\ell + 2)$ both exist in F and have entry 1, yielding a type B coinversion triple in F , so we have $\alpha_\ell = \beta_\ell$. It is also true that the cell $(r, \beta_\ell + 1)$ exists in F and has entry 1. Note that $F(\ell, \beta_\ell) > 1$ unless (ℓ, β_ℓ) is the 1-cell in the basement, but this is not possible since then we have a type B coinversion triple in F . Thus, $F(\ell, \beta_\ell) > F(r, \beta_\ell + 1)$, which entails $F(\ell, \beta_\ell) > F(r, \beta_\ell)$ since otherwise we have a type B coinversion triple in F . By case 2b of Lemma 3.3, we have $F(\ell, i) > F(r, i)$ for all $0 \leq i \leq \beta_\ell$, which implies $\sigma(\ell) > \sigma(r)$ and also that all type A triples within columns ℓ and r in F' are inversion.

Conversely, for each β that is σ -extendable to α , each filling $F' \in \text{SSAF}_\sigma(\beta)$ with no 1-cells (other than the basement) may be extended to a filling F by adding $\alpha_i - \beta_i$ 1-cells above each column $i \in [n]$ in F' . We prove $F \in \text{SSAF}_\sigma(\alpha)$ by again considering two columns at a time; let $1 \leq \ell < r \leq n$.

1. If $\alpha_\ell \geq \alpha_r$ and $\beta_\ell \geq \beta_r$, then $\alpha_r \leq \beta_\ell$. We only need to confirm that type A triples containing a 1-cell within columns ℓ and r in F are inversion. If column ℓ contains the 1-entry in the basement, then $\beta_\ell = 0$, so $\alpha_r = 0$, and there are no type A triples to check. Otherwise, since $\alpha_r \leq \beta_\ell$, the 1-cells in column ℓ occur at a height greater

than α_r and thus are not in a type A triple within these columns. Further, all type A triples with a 1-cell in column r contain two cells in column ℓ with entries greater than 1, so these triples are inversion.

2. If $\alpha_\ell < \alpha_r$ and $\beta_\ell < \beta_r$, then $\alpha_\ell < \beta_r$. We only need to confirm that type B triples containing a 1-cell within columns ℓ and r in F are inversion. Since $\alpha_\ell < \beta_r$, any 1-cells in column r occur at a height greater than $\alpha_\ell + 1$ and thus are not in a type B triple within these columns. Further, all type B triples with a 1-cell in column ℓ contain two cells in column r which have entries greater than 1, so these triples are inversion.
3. If $\alpha_\ell \geq \alpha_r$ and $\beta_\ell < \beta_r$, then $\alpha_r = \beta_r$ and $\sigma(\ell) < \sigma(r)$. Note that F contains no 1-cells in column r since $\sigma(r) > 1$ and $\alpha_r = \beta_r$. Since $\sigma(\ell) < \sigma(r)$, by case 2a of Lemma 3.3, we have $F(\ell, i) < F(r, i + 1)$ for all $0 \leq i \leq \beta_\ell$, yielding type A inversion triples $(\ell, i + 1), (r, i + 1), (\ell, i)$. The remaining type A triples in F contain two adjacent 1-cells in column ℓ and are inversion since column r contains no 1-cells.
4. If $\alpha_\ell < \alpha_r$ and $\beta_\ell \geq \beta_r$, then $\alpha_\ell = \beta_\ell$ and $\sigma(\ell) > \sigma(r)$. Note that F contains no 1-cells in column ℓ since $\sigma(\ell) > 1$ and $\alpha_\ell = \beta_\ell$. Since $\sigma(\ell) > \sigma(r)$, by case 1b of Lemma 3.3, we have $F(\ell, i) > F(r, i)$ for all $0 \leq i \leq \beta_r$, yielding type B inversion triples $(r, i + 1), (\ell, i), (r, i)$. The remaining type B triples contain two adjacent 1-cells in column r and are inversion since column ℓ contains no 1-cells.

To finish the proof, note that the sum of the monomials $x^{F'}$ over all $F' \in \text{SSAF}_\sigma(\beta)$ where the only 1-entry is in the basement is $\mathcal{A}_\beta^\sigma(0, x_2, \dots, x_n)$. The factor $x_1^{|\alpha| - |\beta|}$ accounts for appending $|\alpha| - |\beta|$ cells with entry 1 to each of these fillings. \square

Corollary 3.5. *Using the σ -extendable relation, we can define a poset on weak compositions, which is ranked by length, given by a covering relation \leq_σ . Atoms may be written as summations over saturated chains in this poset, given by*

$$\mathcal{A}_\alpha^\sigma(x) = \sum_{\beta_{(n)} \leq_\sigma \dots \leq_\sigma \beta_{(1)} \leq_\sigma \alpha} x_1^{|\alpha| - |\beta_{(1)}|} x_2^{|\beta_{(2)}| - |\beta_{(1)}|} \dots x_n^{|\beta_{(n)}| - |\beta_{(n-1)}|}.$$

Proof. Set $\sigma_0 := \sigma$ and, for $1 \leq i \leq n$, construct permutations σ_i by deleting 1 from σ_{i-1} and then subtracting 1 from the remaining entries. Set $s_i = \sigma_i^{-1}(1)$. We say $\beta \leq_\sigma \alpha$ if $(\beta_1, \dots, \beta_{s_k-1}, 0, \beta_{s_k+1}, \dots, \beta_n)$ is σ_k -extensible to α , where $k = n - \text{len}(\beta) - 1$. This

poset is ranked by length since $\text{len}(\beta) = \text{len}(\alpha) - 1$. Next, consider the expansion from Theorem 3.4:

$$\mathcal{A}_\alpha^\sigma(x) = \sum_{\beta \text{ } \sigma\text{-extendable to } \alpha} x_1^{|\alpha|-|\beta|} \mathcal{A}_\beta^\sigma(0, x_2, \dots, x_n).$$

If $\beta_{s_0} > 0$, then β does not contribute to this sum, so assume $|\beta_{s_0}| = 0$. Then we have that $\mathcal{A}_\beta^\sigma(0, x_2, \dots, x_n) = \mathcal{A}_{\beta_{(1)}}^{\sigma_1}(x_2, \dots, x_n)$ where the weak composition $\beta_{(1)}$ is obtained by deleting part s_0 from β and σ_1 is obtained by deleting 1 from σ and subtracting 1 from the remaining entries, that is, $\beta_{(1)} \triangleleft_\sigma \alpha$. Noting that $|\beta_{(1)}| = |\beta|$, we recursively expand $\mathcal{A}_\alpha^\sigma(x)$ as

$$\begin{aligned} \mathcal{A}_\alpha^\sigma(x) &= \sum_{\beta_{(1)} \triangleleft_\sigma \alpha} x_1^{|\alpha|-|\beta_{(1)}|} \mathcal{A}_{\beta_{(1)}}^{\sigma_1}(x_2, \dots, x_n) \\ &= \sum_{\beta_{(n)} \triangleleft_\sigma \dots \triangleleft_\sigma \beta_{(1)} \triangleleft_\sigma \alpha} x_1^{|\alpha|-|\beta_{(1)}|} x_2^{|\beta_{(2)}|-|\beta_{(1)}|} \dots x_n^{|\beta_{(n)}|-|\beta_{(n-1)}|}. \end{aligned}$$

□

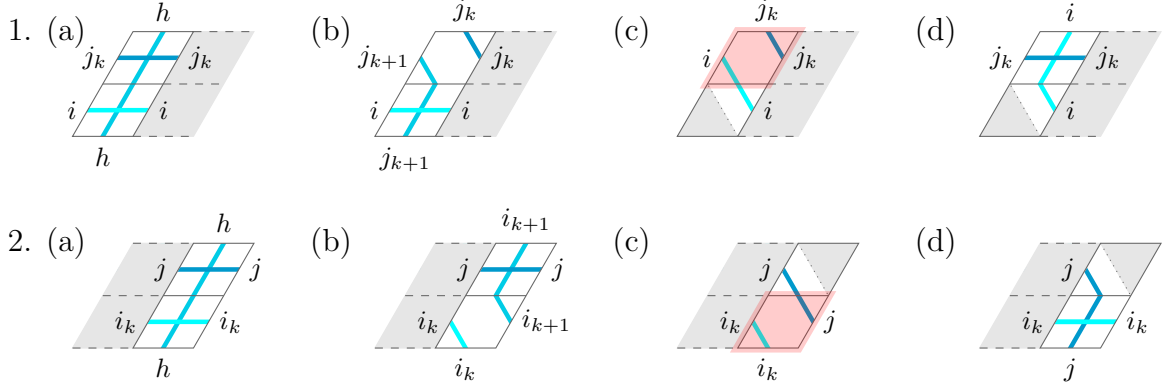
4 Equivalence of models and bijection with skyline fillings

We show that our atom model satisfies Theorem 3.4, which also gives a clear bijection with skyline fillings. We call a string of non-negative integers a **descending string** if it does not contain the substring ij for two positive integers $i < j$. Note that, by our encoding procedure, α^* is a descending string.

Lemma 4.1. *Descending strings label both sides of a column within a legal filling of the atom model (moving up).*

Proof. Descending strings label the left and right boundaries. Assume that there is a descending string between two columns, so there is a position in this vertical where colour i is directly below j and $i < j$. Let $i_0 := i$ and $j_0 := j$.

We consider filling to the left in case 1 and filling to the right in case 2, both situations leading to subcases:



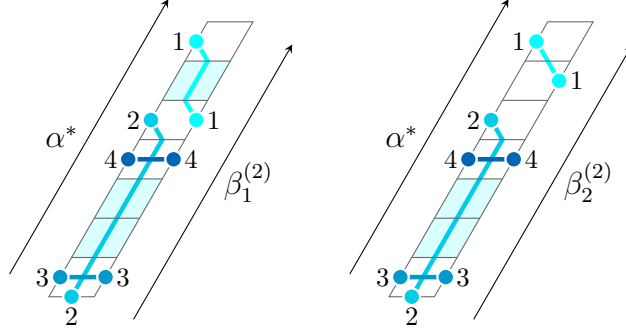
Case 1a transmits i and j_k to the left in the same order. In 1b, we must have $j_{k+1} > j_k > i$. A sequence of cases 1a and 1b then transmits some non-descending string containing ij_k for $i < j_k$ to the left, which cannot continue perpetually since the left boundary is descending. The highlighted tile in 1c is not possible since we maintain $i < j_k$. If 1d occurs after a case of 1b, then line i crosses the same line j_k horizontally and vertically, which is not possible. Thus, it is only possible that case 1d occurs after some sequence of cases 1a and line $i = i_0$ crosses line $j = j_0$. A similar argument forces line i and j to cross twice, which is not possible. Thus, intermediate verticals are also descending strings. \square

We show that the first column in the atom model essentially sums over all β that are σ -extendable to α , proving our models satisfy Theorem 3.4, yielding the same polynomials $\mathcal{A}_\alpha^\sigma(x)$. Note that the first column of a filling contains n colours on its left side, $n - 1$ colours on its right side and the label $s = \sigma^{-1}(1)$ is on the bottom. Lemma 4.1 shows that we may assume the right side of the first column of a filling encodes a weak composition in a way similar to our encoding procedure in Section 2, only skipping over the label s . More technically, the right side encodes a weak composition β , where we assume $\beta_s = 0$, with a new string $\beta^{(s)}$, which is obtained by deleting the character s from β^* and appending 0 to the end.

Example 4.2. Let $\alpha = (3, 2, 0, 2)$ and $\sigma = 4123$, so that $\sigma^{-1} = 2341$ and $s = \sigma^{-1}(1) = 2$. There are two weak compositions $\beta_1 = (2, 0, 0, 2)$ and $\beta_2 = (3, 0, 0, 2)$ which are σ -extendable to α . These correspond to the only two ways of filling the first column with

descending strings on the right. We compute the boundary strings:

$$\begin{array}{lll} \alpha^* = 3004201 & \beta_1^* = 3200410 & \beta_1^{(2)} = 3004100 \\ & \beta_2^* = 3200401 & \beta_2^{(2)} = 3004010 \end{array}$$



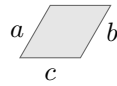
Lemma 4.3. *The first column in the atom model is possible to fill if and only if $\beta^{(s)}$ labels its right side, where $s = \sigma^{-1}(1)$ and β is σ -extendable to α .*

Proof. We have argued above that we may assume the right side of the first column always encodes a weak composition β , where $\beta_s = 0$, with the string $\beta^{(s)}$. We must show that it is possible to fill if and only if β is σ -extendable to α . Note that both strings α^* and $\alpha^{(s)}$ will have α_i instances of the character 0 before the character i , determining the size of part i . Suppose that it is possible to fill the first column and let $1 \leq \ell < r \leq n$.

1. If $\alpha_\ell \geq \alpha_r$ and $\beta_\ell \geq \beta_r$, then the label r occurs below the label ℓ on the left side. If $\ell = s$, then $\beta_\ell = \beta_r = 0$ and line ℓ begins on the bottom side of the column and crosses line r . Then $\alpha_r = \beta_r = 0$ and thus $\alpha_r \leq \beta_\ell$. Otherwise, lines ℓ and r do not cross. Let $i \leq r$ be the smallest integer where $\alpha_i = \alpha_r$ and $j \geq \ell$ be the largest integer where $\beta_j = \beta_\ell$. If line i exits on the left at height h , then line j must exit on the right at height at least h , which implies $\alpha_r \leq \beta_\ell$.
2. If $\alpha_\ell < \alpha_r$ and $\beta_\ell < \beta_r$, then the label ℓ occurs below r on both sides of the column and the lines do not cross. Let $i \leq \ell$ be the smallest integer where $\alpha_i = \alpha_\ell$ and $j \geq r$ be the largest integer where $\beta_j = \beta_r$. If line i exits on the left at height h , then line j must enter on the right at a height $h' \geq h + 1$ and there must be a 0 between height h and h' on the right, which implies $\alpha_\ell < \beta_r$.
3. If $\alpha_\ell \geq \alpha_r$ and $\beta_\ell < \beta_r$, we have $r \neq s$ since $\beta_r > 0$; thus, line r must cross horizontally over line ℓ , so $\alpha_r = \beta_r$ and $\sigma(\ell) < \sigma(r)$.

4. If $\alpha_\ell < \alpha_r$ and $\beta_\ell \geq \beta_r$, suppose $\ell = s$; then $\beta_r = 0$. Line ℓ must cross vertically under all lines $i \geq \ell$ where $\alpha_i = 0$, so $\alpha_r \leq \alpha_\ell$, contradicting our assumptions. Otherwise, line ℓ must cross horizontally over line r , so $\alpha_\ell = \beta_\ell$ and $\sigma(\ell) > \sigma(r)$.

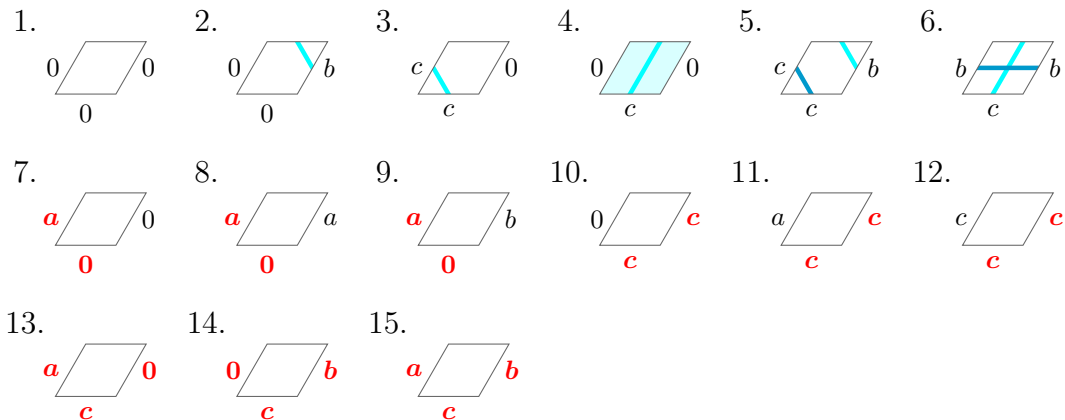
Conversely, suppose β is σ -extendable to α , label the left of a column with α^* and the right with $\beta^{(s)}$. We show that it is always possible to fill this column, considering tiles from the bottom up. The left, right and bottom edges of the tile will have labels a, b, c , determined by the side strings and the previous tile:



Let the current tile be at height h . Let $L(h)$ be the number of 0's below height h on the left side of the column and let $R(h)$ be the number of 0's below height h on the right side. If a and b are positive integers, we have $\alpha_a = L(h)$ and $\beta_b = R(h)$ respectively. We say the **zero condition** is satisfied at height h when

$$L(h) = \begin{cases} R(h) - 1 & \text{if } c = 0 \\ R(h) & \text{if } c > 0. \end{cases}$$

The zero condition is satisfied when $h = 1$, where $c = s > 0$ and $L(h) = R(h) = 0$; by induction, assume it is satisfied at height $h - 1 \geq 1$. Let a, b and c be distinct positive integers. There are 15 cases for the tile at height h :



We have emphasized problematic clusters of labels in bold red font. We want to show that only cases 1-6 are possible and a tile may always be placed in these cases; this will also ensure we satisfy the zero condition at height $h + 1$.

- 1-4. It is always possible to place a tile in these cases.
5. We must show that $b < c$ to have a valid tile; suppose $c < b$. Then line b exits on the left at a height above h and, since α^* is a descending string, we must have $\alpha_c < \alpha_b$. We must also have that $\beta_c \leq \beta_b$; if $c = s$ and $\beta_c = \beta_b$, we have that $\sigma(c) > \sigma(b)$ by case 4 of Definition 3.2, which is not possible since $\sigma(c) = 1$. Otherwise, $c = s$ and $\beta_c < \beta_b$ or $c \neq s$, and we still have $\beta_c < \beta_b$ since $\beta^{(s)}$ is a descending string. By case 2 of Definition 3.2, we have that $\alpha_c < \beta_b$, but $\alpha_c = L(h) = R(h) = \beta_b$; hence, $b < c$.
6. For the crossing to occur, we must show $\sigma(c) < \sigma(b)$. If $c = s$, then $\sigma(c) = 1 < \sigma(b)$, as desired. Otherwise, if $c < b$, then $\alpha_c \geq \alpha_b$ and $\beta_c < \beta_b$, so $\sigma(c) < \sigma(b)$ by case 3 of Definition 3.2. If $b < c$, then $\alpha_b < \alpha_c$ and $\beta_b \geq \beta_c$, so $\sigma(b) > \sigma(c)$ by case 4 of Definition 3.2.
- 7-9. These cases cannot occur since then line a enters on the right at height at least h ; since $L(h) < R(h)$, we have $\alpha_a < \beta_a$.
- 10-12. These cases cannot occur since then line c enters the column on the bottom or right twice, which is not possible.
13. Since we assume $\alpha_a = L(h) = R(h)$ and the right label is 0, this case implies $\alpha_a < \beta_a$.
14. We have that α_b and α_c are greater than both β_b and β_c because of the 0 on the left. Thus, we cannot satisfy Definition 3.2 since each case implies $\alpha_d \leq \beta_e$ for at least one pair $d, e \in \{b, c\}$.
15. This case implies line a must enter on the right side at a height above h . This is only possible if $\beta_a = \beta_b$ and $a < b$, otherwise $\alpha_a < \beta_a$. On the left side, labels b and c must be above a , so we have $\alpha_b \geq \alpha_a$ and $\alpha_c \geq \alpha_a$.

We cannot have that $\alpha_b = \alpha_a$ since $a < b$, so $\alpha_a < \alpha_b$. If $\alpha_c = \alpha_a$, then $c < a < b$ and $\alpha_c < \alpha_b$; note that $\beta_c \leq \beta_b$. If $\beta_c < \beta_b$, then by case 2 of Definition 3.2, we have $\alpha_c < \beta_b$, meaning c must have exited at a previous step. If $\alpha_c = \alpha_b$, we are in case 4 of Definition 3.2 and $\sigma(c) > \sigma(b)$, meaning it is not possible that $c = s$; otherwise, $\alpha_c = \beta_c$, meaning $\beta_c = \beta_b$, which is not possible since $\beta^{(s)}$ is a descending string.

Thus, $\alpha_b > \alpha_a$ and $\alpha_c > \alpha_a$, implying that α_b and α_c are both greater than β_b and β_c , and we cannot satisfy Definition 3.2 for the same reason as in case 14.

□

We now justify that our atom model yields the same polynomials as those given in terms of SSAFs in Section 3.

Theorem 4.4. *The polynomials given by the atom model satisfy Theorem 3.4.*

Proof. By Lemma 4.3, we can consider a sum over β that are σ -extendable to α . The converse in Lemma 4.3 also shows that there is only one filling of the first column for each such β since there is only one way to fill each tile. The number of nontrivial tiles each line $i \in [n]$ moves through is $\alpha_i - \beta_i$, so the weight of a filling of the first column is $x_1^{|\alpha| - |\beta|}$.

Consider the atom model for $\mathcal{A}_\beta^\sigma(x_1, \dots, x_n)$ and set $x_1 = 0$. The fillings that contribute will have weight 1 in the first column, force line s to exit at the bottom and encode $\beta^{(s)}$ on the right. Then columns $2, \dots, n$ are filled as if there is no first column, showing

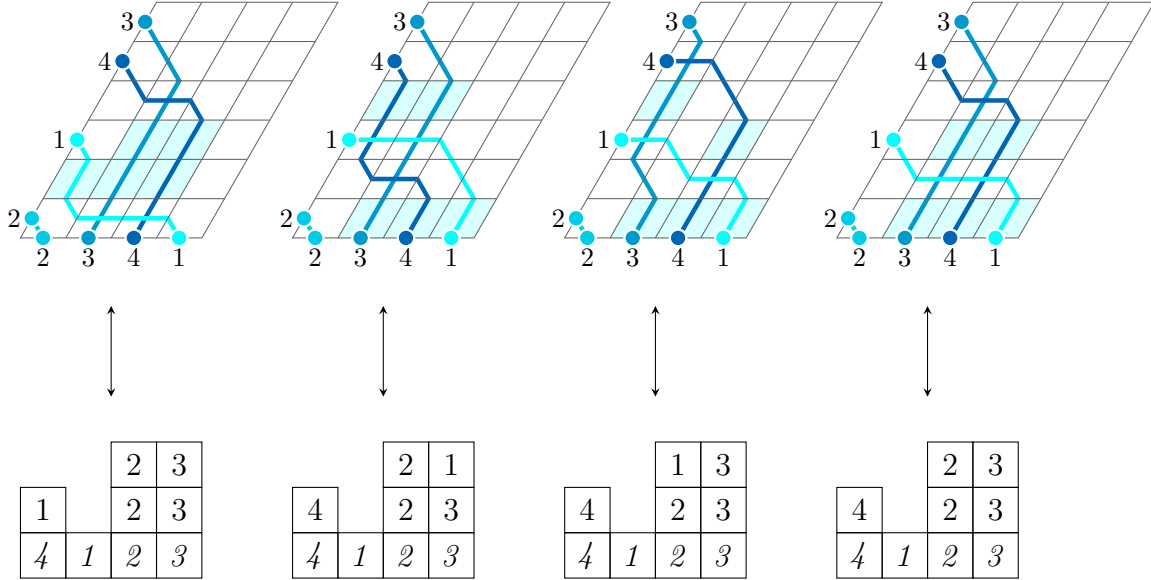
$$\mathcal{A}_\alpha^\sigma(x) = \sum_{\beta \text{ } \sigma\text{-extendable to } \alpha} x_1^{|\alpha| - |\beta|} \mathcal{A}_\beta^\sigma(0, x_2, \dots, x_n).$$

□

As in [7], we may obtain the SSAF corresponding to a filling of the atom model by simply following line i to produce the entries in column i . This is relatively clear in light of Theorem 4.4 using induction. The inverse map is technical to state and we omit it.

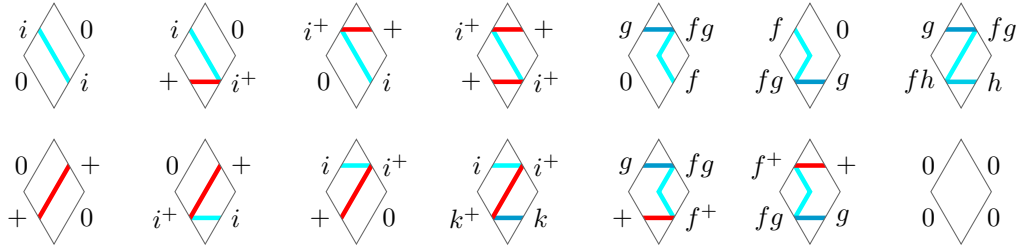
Begin with a skyline diagram of shape α with basement σ and other entries blank. In a filling of the atom model, follow line i from the bottom, moving up. Each time i moves through a nontrivial tile within a column c , we assign the entry c to the bottom-most blank entry of column i in the skyline diagram.

Example 4.5. We show the corresponding SSAFs for the fillings in Example 2.2 where $\alpha = (1, 0, 2, 2)$ and $\sigma = 4123$, so $\sigma^{-1} = 2341$ and $\alpha^* = 201043$. Note that columns in SSAFs are numbered 1 to n from left to right. Columns are not numbered by their basement entries.



5 Vertex models for $a_{\alpha\lambda}^\beta(\sigma)$

We give vertex models for the structure coefficients $a_{\alpha\lambda}^\beta(\sigma)$. Our models use the “diamond” tiles below where f, g, h, i are in $[n]$, $\sigma(f) < \sigma(g)$ and $\sigma(f) < \sigma(h)$. The label b^+ indicates a blue line b and a red line share that edge. The label ab indicates two shades of blue a and b with $\sigma(a) < \sigma(b)$ share that edge. All tiles have weight 1.



Further, we do not allow two adjacent tiles to form an internal rhombus, as depicted in Figure 5.1. These restrictions are still local and can be imposed with additional labels (see Appendix A), but we exclude them to avoid clutter. We may now state our theorem.

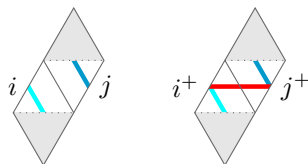
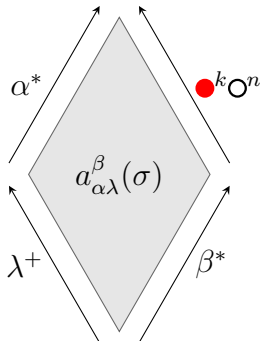


Figure 5.1: Banned adjacencies where $1 \leq i < j \leq n$.

Theorem 5.2. *The structure coefficients $a_{\alpha\lambda}^{\beta}(\sigma)$ are given by the partition function of the model*

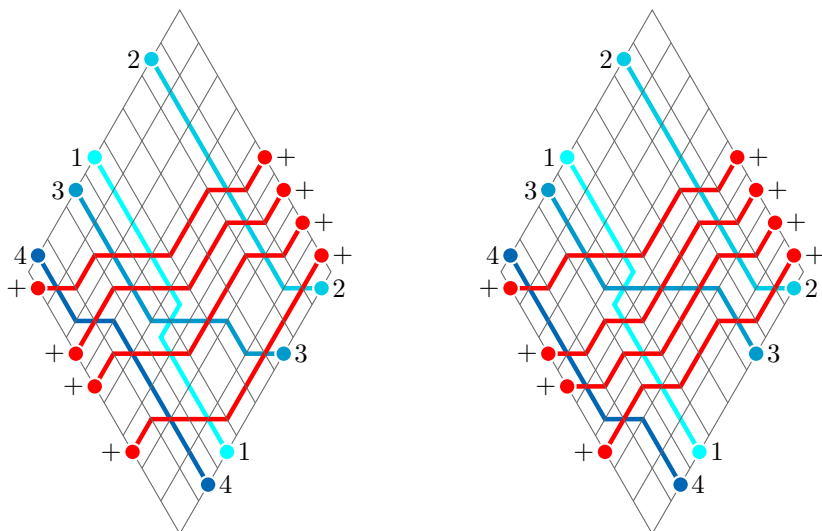


where $k = \max(\beta)$ and the restrictions in Figure 5.1 apply respectively within. The symbol $\bullet^k 0^n$ represents the string $+^k 0^n$.

We call our vertex model for $a_{\alpha\lambda}^{\beta}(\sigma)$ the *atom-Schur model*. Recall that we assume α , β and λ have length n , but we may append zeros to match their lengths. Similarly, we may append zeros to the end of the string α^* and append $+$ symbols to the end of λ^+ so that these strings all have length $n + k$.

Remark 5.3. The diamonds may be cut in half because the top half is always fixed, giving a triangular puzzle rule as in [20, 21, 22, 32, 33].

Example 5.4. For $\alpha = (1, 3, 1, 0)$, $\lambda = (3, 1, 0, 0)$ and $\beta = (1, 4, 3, 1)$, we have $k = \max(\beta) = 4$. If $\sigma(1) < \sigma(3)$, there are two fillings of the atom model, showing $a_{\alpha\lambda}^{\beta}(\sigma) = 2$, otherwise $a_{\alpha\lambda}^{\beta}(\sigma) = 0$.

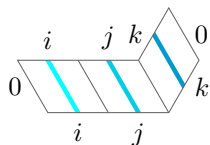


6 Proof of Theorem 5.2

We combine the three models in one picture to show Theorem 5.2. The crucial machinery for this proof is an analogue of the Yang–Baxter equation, which we refer to as the Column Lemma 6.3. New tiles are necessarily, expanding the previous set and introducing a new orientation.

Figure 6.1 depicts the complete set of tiles. We call the tiles in the first row *right-sheared*, the tiles in the second row *left-sheared* and the tiles in the third row *diamonds*. The left-sheared tiles contain a new nontrivial tile of weight $-x_c$. We again depict vertex models with grey diagrams filled with tiles of matching orientation. Left- and right-sheared tiles share the same column number c if one is on top of the other; columns are numbered 1 to n from left to right. Note that red lines may now travel alongside blue lines; these tiles facilitate the proof, but they can be excluded in Theorem 5.2.

We still ban internal rhombi between diamond tiles as in Figure 5.1, but there are no restrictions between tiles that are not both diamonds. Left-sheared tiles are unaffected; for example, the following configuration where $1 \leq i < j < k \leq n$ is legal:



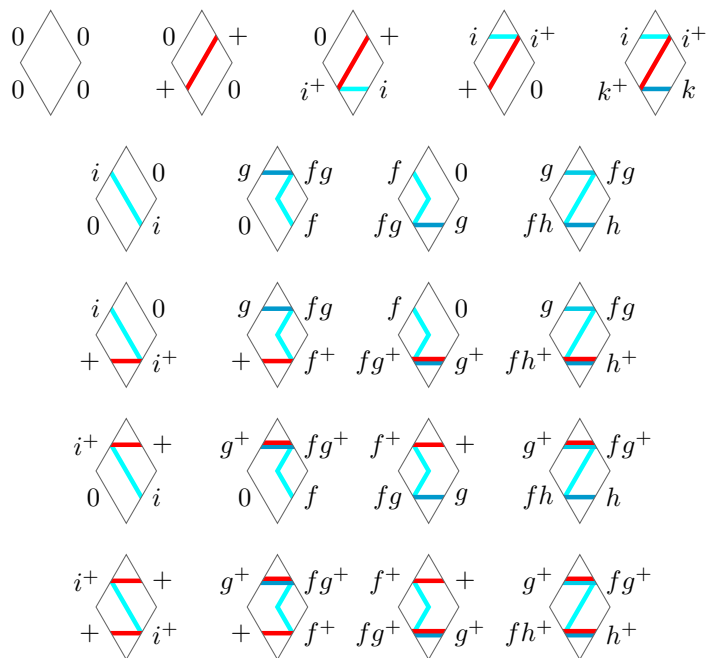
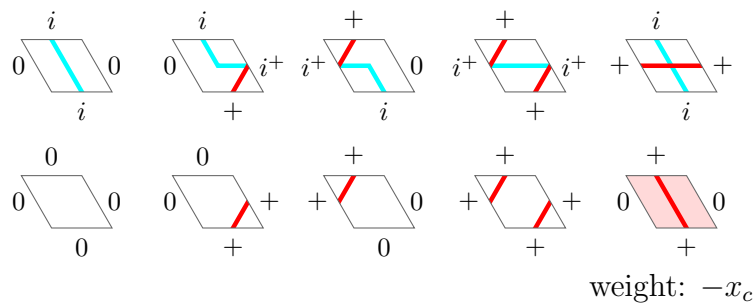
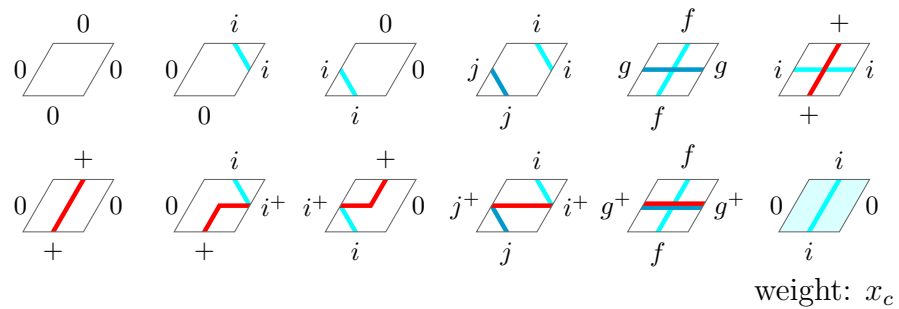
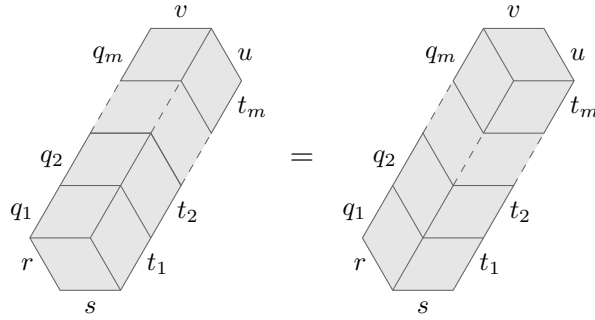


Figure 6.1: The full set of tiles where f, g, h, i, j, k are in $[n]$, $i \leq j$, $\sigma(f) < \sigma(g)$ and $\sigma(f) < \sigma(h)$.

Note 6.2. The diamond tiles are determined by cutting all trivial right-sheared tiles into triangles and gluing them together in all possible ways. This introduces new labels responsible for the restrictions in Figure 5.1. We suppress these extra labels to clean up analysis but show them in Appendix A. The left-sheared tiles are not determined this way and do not allow crossings between blue lines.

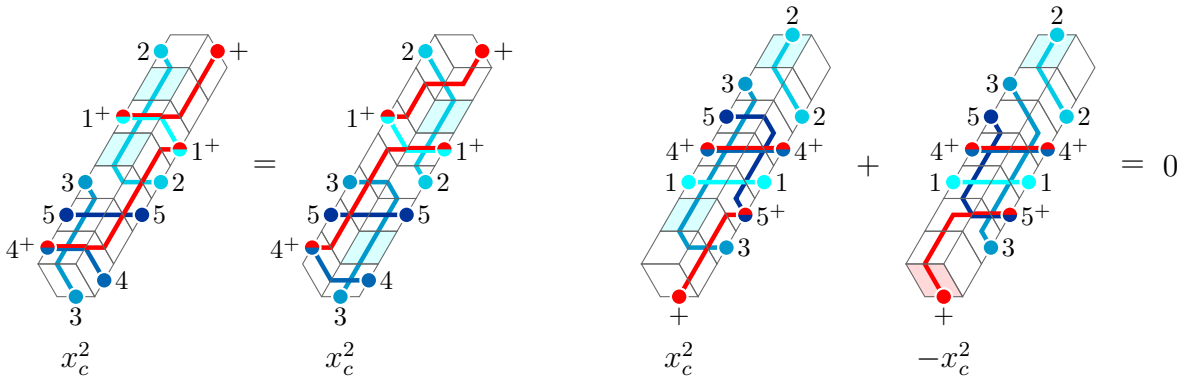
The key to our proof is the following lemma equating columns of tiles.

Lemma 6.3 (The Column Lemma). *Let $q_1, \dots, q_m, r, s, t_1, \dots, t_m, u, v$ be fixed labels where r and u are in $\{0, +\}$. The following equality holds:*



Proof. We reserve this proof for Section 7. □

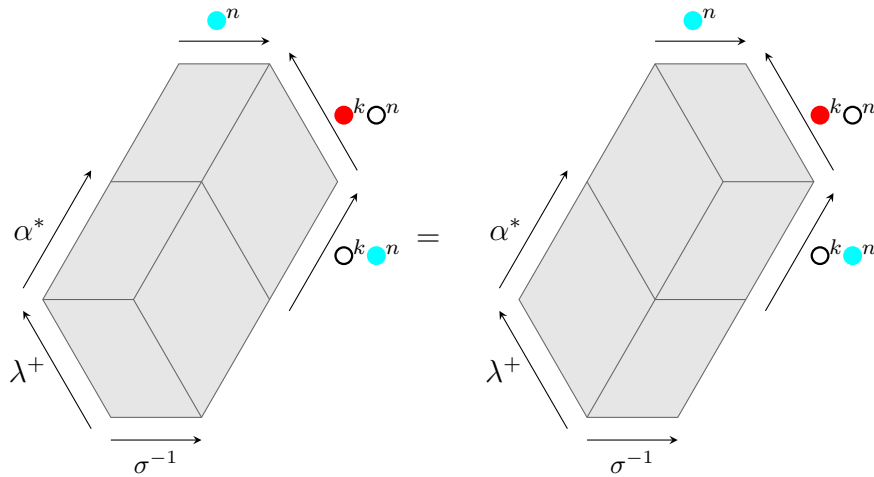
Example 6.4. We consider two examples of Lemma 6.3. In the first example, both sides have weight x_c^2 . In the second, there are two ways to fill the column on the left-hand side which cancel, and there is no way to fill the column on the right-hand side.



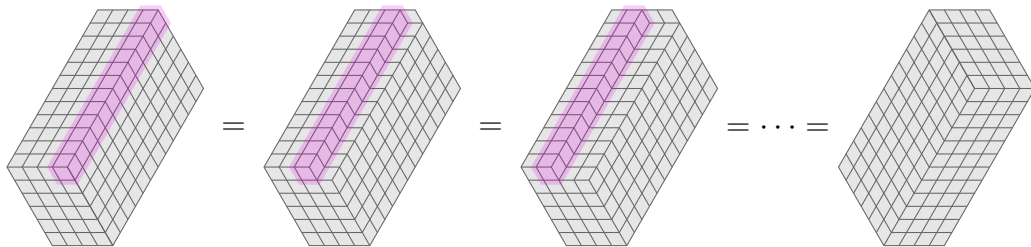
Remark 6.5. The tiles in Figure 6.1 are minimal in the sense that Lemma 6.3 does not hold if we remove any tile. In [32, 33], the authors proceed similarly with a Yang–Baxter equation that equates unit hexagons with unrestricted boundaries. In contrast, our equation restricts the labels on the southwest and northeast edges, suggesting a more general framework to explore.

Interpreting the next lemma proves our result.

Lemma 6.6. Set $k = \max(\alpha) + \max(\lambda)$. The configurations below have the same weight:



Proof. Repeatedly applying the Column Lemma 6.3 to internal columns of length $2(k+n)$, from right to left, top to bottom, shows equality. We illustrate this schematically, omitting the boundaries:



The boundary conditions ensure that the southwest and northeast labels of columns we equate are always in $\{0, +\}$ at every stage in this process, allowing repetition of Lemma 6.3. \square

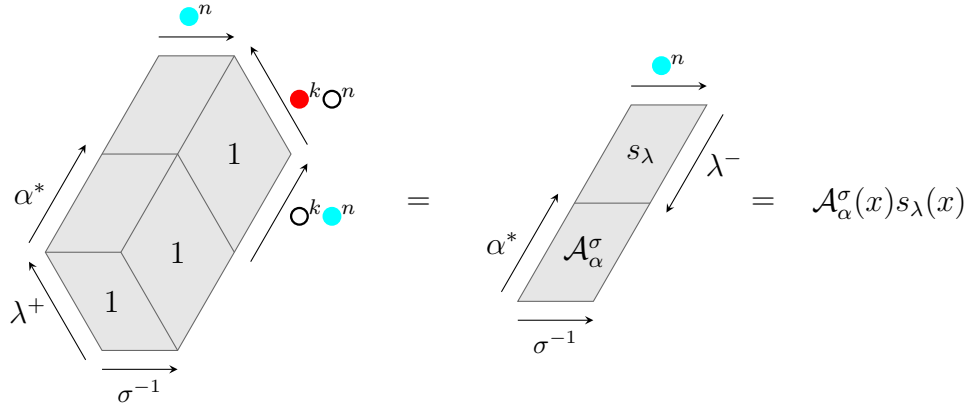
The proof now follows from examining both sides of the equation in Lemma 6.6. In short, the left-hand side is manifestly the product $\mathcal{A}_\alpha^\sigma(x)s_\lambda(x)$ and the right-hand side is manifestly the summation $\sum_\beta a_{\alpha\lambda}^\beta(\sigma)\mathcal{A}_\alpha^\sigma(x)$ where $a_{\alpha\lambda}^\beta(\sigma)$ is the partition function of the atom-Schur model.

Proof of Theorem 5.2. Before proceeding, we note a few differences with our main theorem:

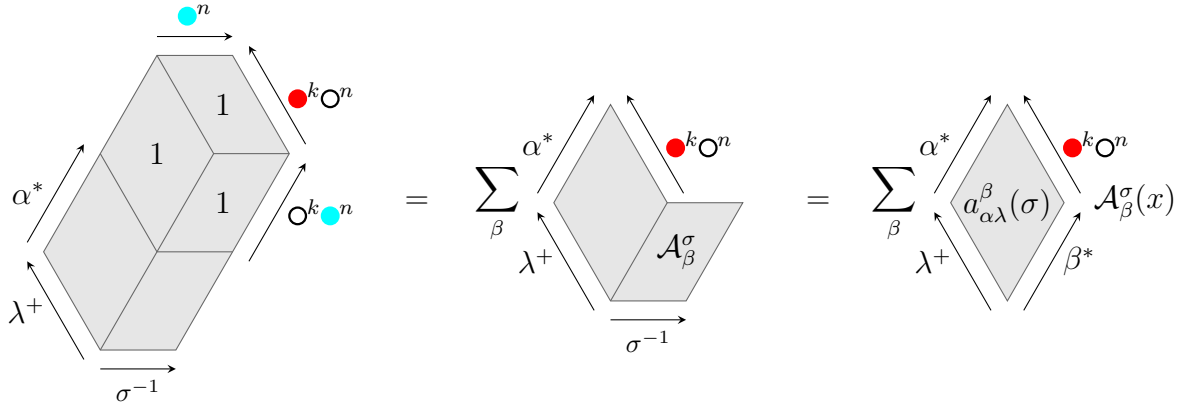
1. Here, we include diamond tiles, where blue lines travel alongside red lines, to facilitate the proof. These will not occur in the atom-Schur model, so we omit them in Theorem 5.2.
2. We have set $k = \max(\lambda) + \max(\alpha)$, but when considering the filling of a particular diamond where β is given, it suffices to set $k = \max(\beta)$, as we do in Theorem 5.2.

See the illustration in Figure 6.7 where we label regions **A**, **B**, \dots , **K**. Within region **A**, all blue lines must move northwest and all red lines must move east. The red lines continue straight northeast through **B**, transmitting the string λ^+ to the southwest boundary of **C**. Lemma 10 in [33] says that there is only one way to fill **C**, which forces the shared boundary between **C** and **E** to be the string λ^- upside-down. Thus, regions **A**, **B** and **C** have weight 1.

Next, we recognize region **D** as the atom model $\mathcal{A}_\alpha^\sigma(x)$. From the previous paragraph, we have that λ^- is upside-down on the southeast boundary of **E**. Rotating region **E** by 180 degrees, we see that it is the Schur model for $s_\lambda(x)$ with the variables in reverse order; since $s_\lambda(x)$ is symmetric, the weight of the left-hand side is the product $\mathcal{A}_\alpha^\sigma(x)s_\lambda(x)$. We summarize pictorially:



On the right-hand side, the regions **G**, **H** and **I** always have weight 1 and cross as in Figure 6.7. Within region **J**, all blue lines must exit the northwest boundary if they are to reach the northwest boundary of **K** (our choice of k makes the boundary long enough to ensure this). The blue lines then travel through the boundary between **J** and **K**, varying over strings β^* that encode weak compositions β (these strings will be descending by a similar argument made in Lemma 4.1). For each β^* along this boundary, we recognize region **J** as $\mathcal{A}_\beta^\sigma(x)$ and region **K** as the atom-Schur model from Theorem 5.2. Thus, the right-hand side is a summation over compositions β where each summand is a product of our atom-Schur model and $\mathcal{A}_\beta^\sigma(x)$. Again, summarizing pictorially:



By Lemma 6.6, we can equate both sides, completing the proof. □

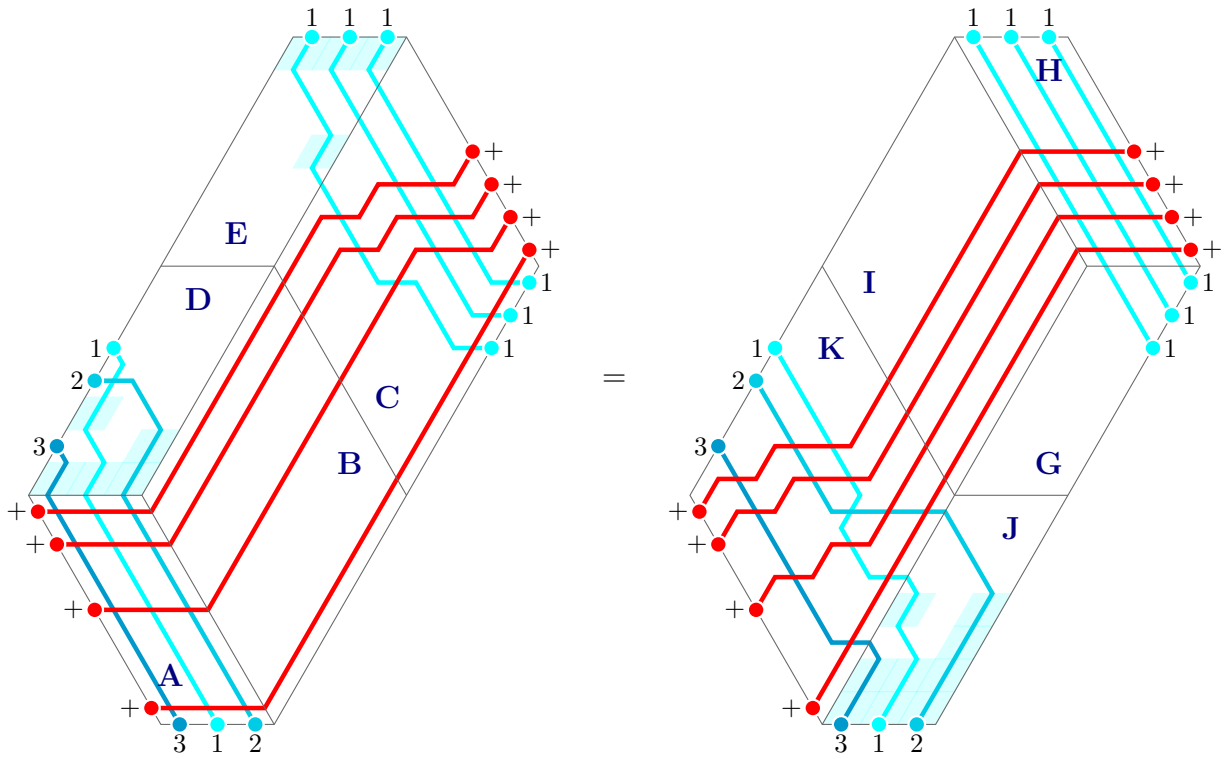
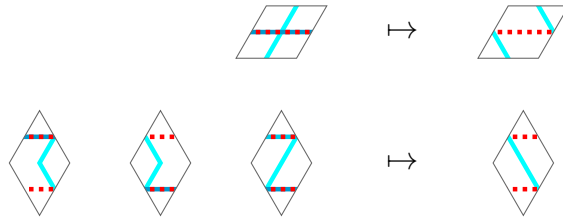


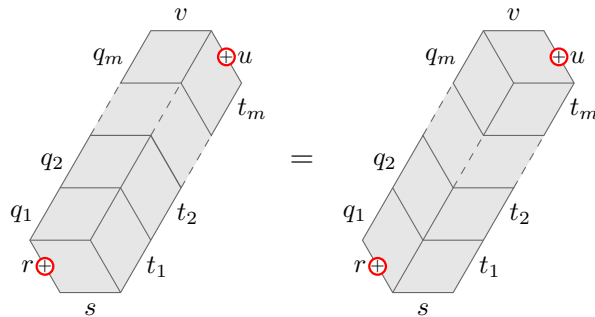
Figure 6.7: Two fillings of weight $x_1^3 x_2^2 x_3^4$ from the configurations in Lemma 6.6 where $\lambda = (2, 2, 1)$, $\sigma = 231$ and $\alpha = (2, 2, 1)$, so that $n = 3$, $k = 4$ and $\sigma^{-1} = 312$. Regions are labelled to facilitate exposition.

7 Proof of the Column Lemma 6.3

We prove the key technical result of this paper, the Column Lemma 6.3. We use diagrams with symbols that indicate restrictions on labels. The symbol \circ indicates the label is 0, \oplus indicates the label is in $\{0, +\}$ and \odot indicates the label is in $\{b, b^+\}$ for $b \in [n]$. We also allow comparison of labels so that if $q \in \{a, a^+\}$ and $t \in \{b, b^+\}$ for $a \leq b$, then $q \leq t$. We set blue labels equal to show the general outline of fillings. Doing this has the effect of uncrossing lines, altering the following tiles (dotted red lines indicate a red line may be present or not):



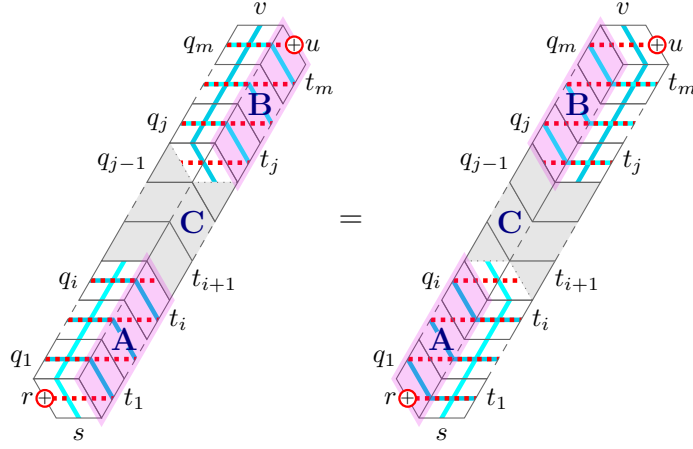
Restating Lemma 6.3 with these conventions, we wish to prove the equation



We first show that Lemma 6.3 is true when both columns use only trivial tiles, that is, when $x_c = 0$.

Lemma 7.1. *Lemma 6.3 is true when $x_c = 0$.*

Proof. As stated in Note 6.2, diamond tiles are produced by taking trivial right-sheared tiles, cutting them into triangles, and gluing them together in all possible ways. Left-sheared tiles behave differently, not allowing crossings. The result is that columns with only trivial tiles are decorated identically unless $s < t_1$ or $v > q_m$. We outline the general case where both of these are true:



In the left column, line s crosses vertically under some contiguous sequence of lines that exit at q_1, \dots, q_i . Let i be the smallest integer where $t_{i+1} = 0$, $t_{i+1} \leq s < q_i$ or $i = m$. Within the right column, line s must turn to the left after exiting the tile labelled by t_i . Similarly, if $v > q_m$, then line v must cross vertically under some contiguous sequence of lines entering at t_j, \dots, t_m where j is the largest value where $q_{j-1} = 0$, $q_{j-1} \leq v < t_j$ or $j = 1$ before turning right within the left-hand filling.

The grey regions **C** are filled identically in both columns. We set $q_1 = \dots = q_i$, and $q_j = \dots = q_m$, but these labels may be different, in which case crossings may occur identically in regions **A** or **B**. \square

We proceed by induction on m . In light of the following lemma, the base case $m = 1$ holds.

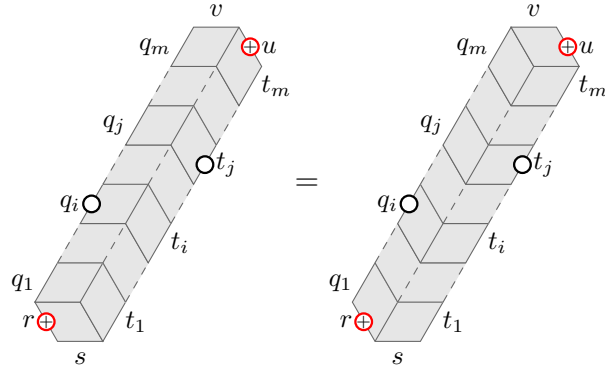
Lemma 7.2. *The unit hexagons with the following restrictions are equivalent:*



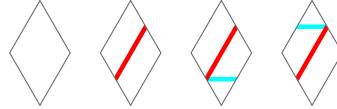
Proof. Both equations follow from brute force. Note that r and u are unrestricted in the second equation. \square

Many cases are now possible to prove by induction.

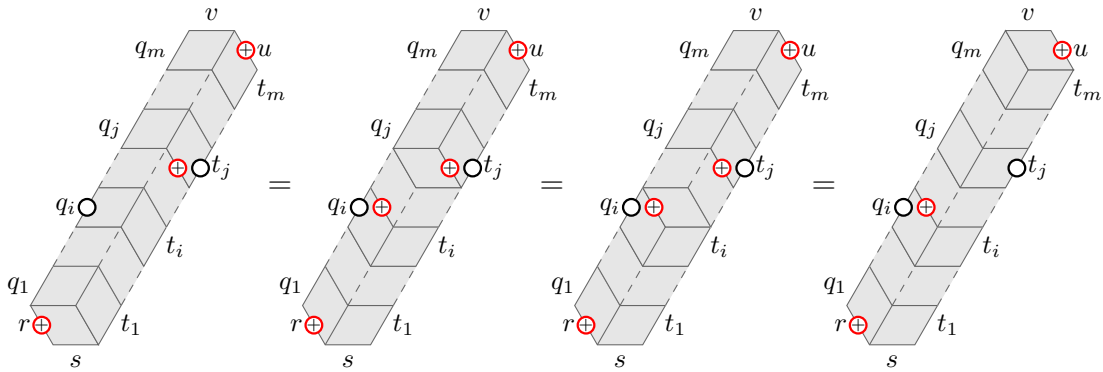
Lemma 7.3. Assume that Lemma 6.3 holds for columns of length $m - 1 \geq 1$. Then if $q_i = t_j = 0$ for $1 \leq i \leq j \leq m$, we have:



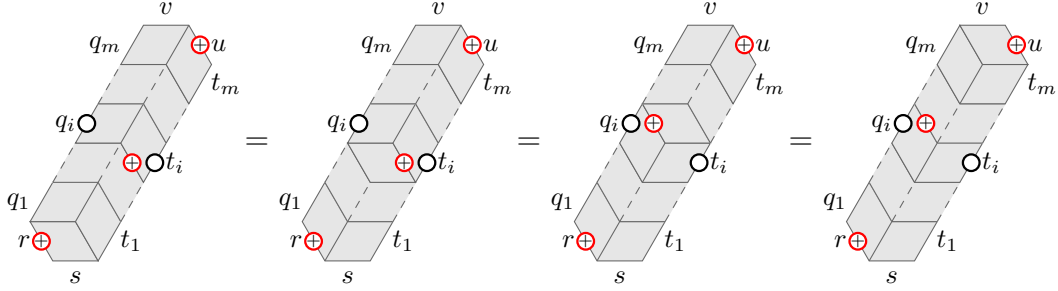
Proof. Note that if the northwest or southeast edge of a diamond tile is 0, then the northeast or southwest edge, respectively, must be in $\{0, +\}$ since these are the only such tiles:



Because of the above note, we know some internal edges are in $\{0, +\}$, which we label with the \oplus symbol. If $i < j$, we have the following equivalences by repeatedly applying Lemma 6.3:



If $i = j$, we have the following equivalences, where the second equivalence follows from applying the second equation in Lemma 7.2:

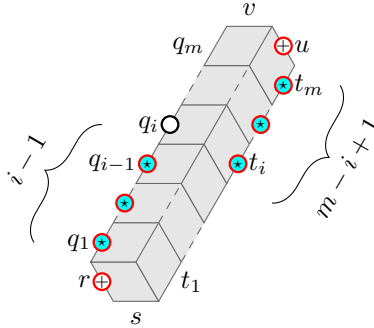


□

Since r and u are in $\{0, +\}$, there can be at most $m + 1$ separate blue lines within a column, entering at s, t_1, \dots, t_m and exiting at v, q_1, \dots, q_m . The next lemma shows that we can assume at least $m - 1$ separate blue lines.

Lemma 7.4. *Lemma 6.3 holds for columns of length m containing less than $m - 1$ separate blue lines.*

Proof. If $q_i \neq 0$ for all $1 \leq i \leq m$, there are at least m separate blue lines within a column. Otherwise, let i be the smallest integer with $q_i = 0$, so there is a blue line at q_k for $1 \leq k < i$. By Lemma 7.3, we can assume that $t_j \neq 0$ for $i \leq j \leq m$. This accounts for $(i - 1) + (m - i + 1) = m$ edges incident with a blue line:

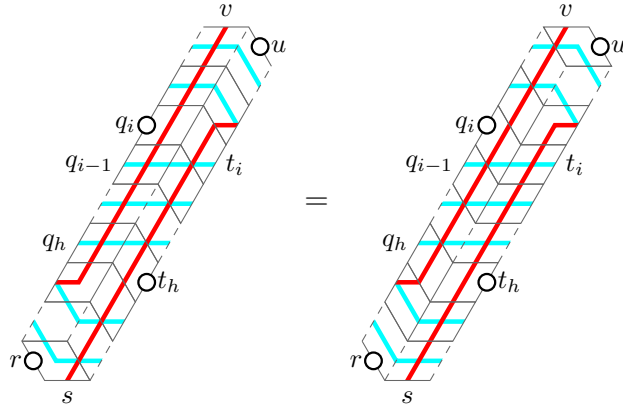


The line entering at t_i may exit at q_{i-1} , but none of the lines entering at t_{i+1}, \dots, t_m may exit at q_1, \dots, q_{i-1} , accounting for at least $m - 1$ separate blue lines. □

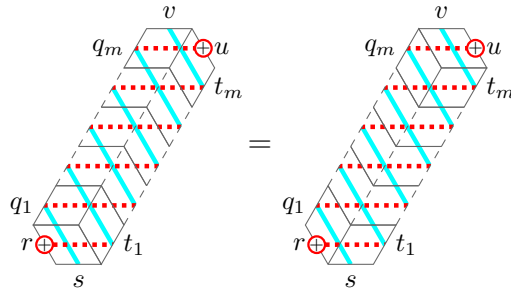
We now prove Lemma 6.3 by handling the remaining cases.

Proof of the Column Lemma 6.3. From Lemma 7.4, we only need to consider the cases of a column with at least $m - 1$ separate blue lines. We again set labels equal, uncrossing blue lines, to show the general structure of fillings.

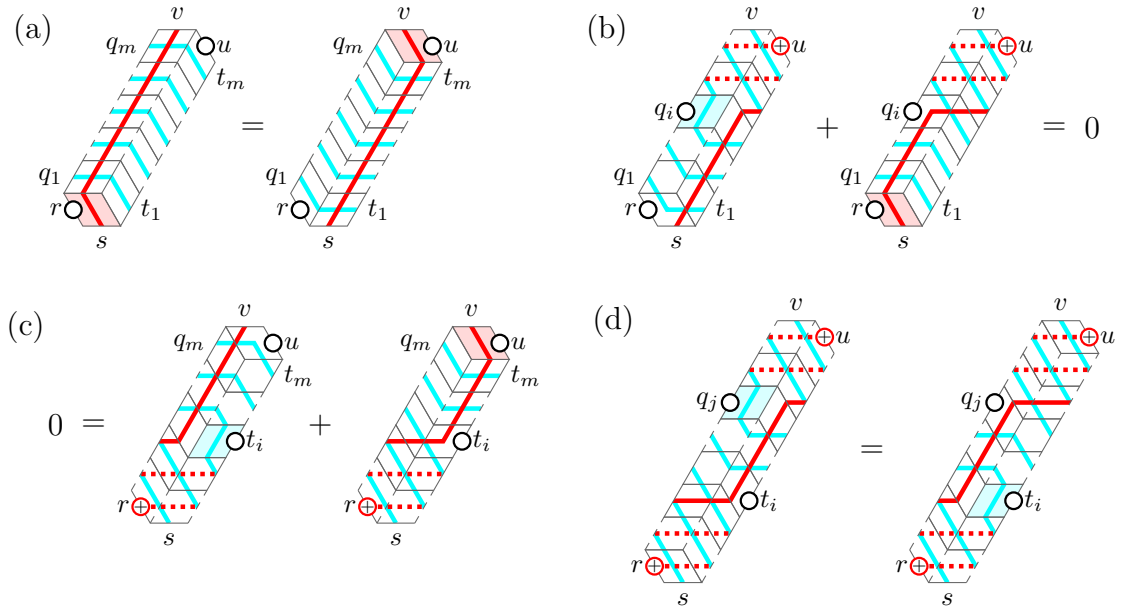
1. If there are $m - 1$ separate blue lines, we have $q_i = 0$ for some $1 \leq i \leq m$. As argued in Lemma 7.4, we can assume t_i, \dots, t_m and q_1, \dots, q_{i-1} are nonzero and a blue line b entering at t_i must exit at q_{i-1} . If b crosses a blue line, we have at least m separate blue lines, so b crosses over two red lines. These cases only use trivial tiles, covered by Lemma 7.1. We give a general outline where $1 \leq h < i \leq m$:



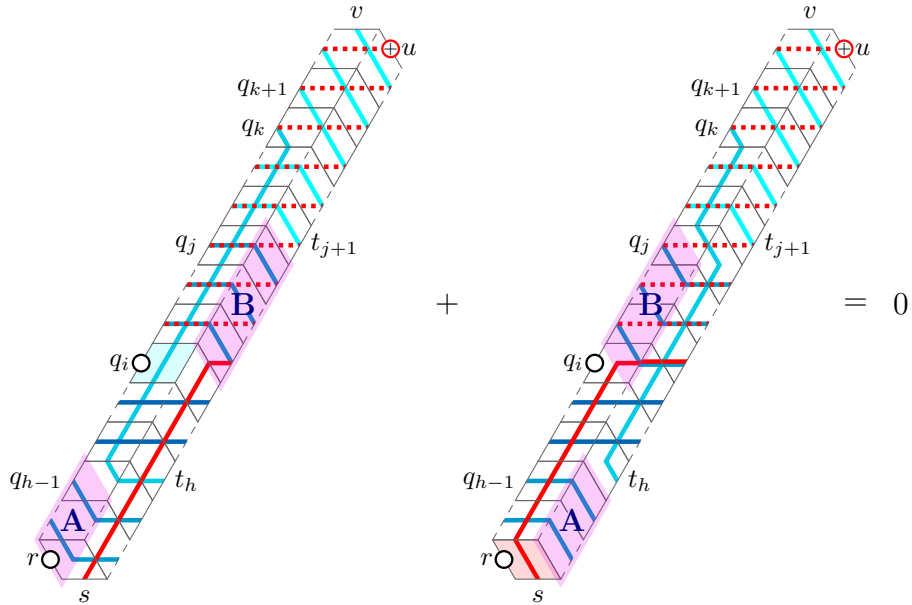
2. If there are $m + 1$ separate blue lines, these cases only use trivial tiles and so are covered by Lemma 7.1:



3. If there are m separate blue lines, there are four outlines using a nontrivial tile.



In each case, allowing different colours preserves equality. Case 3a is clear, though the other cases require more careful analysis and examples can get quite large. We outline case 3b in the most general situation, tracking the blue line in the left filling that passes by $q_i = 0$. Say this line enters at t_h and exits at q_k and let $1 \leq h \leq i < j < k \leq m$:



Here, j is the smallest integer where $q_j < t_h \leq t_{j+1}$; we also require that $q_{h-1} \leq t_h$ and $q_k \leq q_{k+1}$ to fill either column. As before, crossings in regions **A** or **B** will occur identically.

□

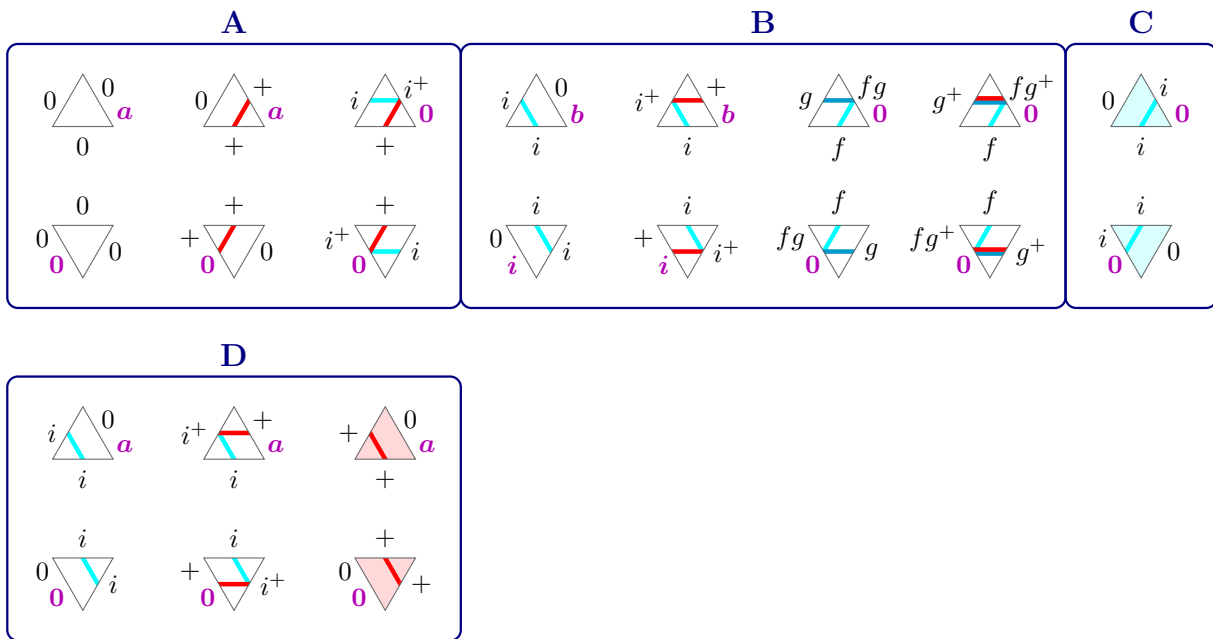
Acknowledgements

I am deeply grateful to Kevin Purbhoo for introducing me to this approach, for many discussions, and for his boundless encouragement over the course of this project. I thank Oliver Pechenik for valuable feedback on the final draft. I thank Allen Knutson and Paul Zinn-Justin for hosting a great workshop on vertex models (LAWRGe 2022), answering some burning questions. Allen also had several comments that led to valuable probing of this framework. This work was supported by Kevin Purbhoo's NSERC Discovery Grants.

Appendix

A Triangle tiles and extra labels

We may add extra labels to our tiles in Figure 6.1 to enforce the restrictions in Figure 5.1 between diamond tiles, only requiring that labels match along edges. We construct rhombic tiles out of triangles with extra labels, emphasized in bold purple font.



Here, $i, f, g \in [n]$, $\sigma(f) < \sigma(g)$, $0 \leq a \leq n$ and $0 \leq b \leq i$. Rhombic tiles only use a subset of triangular tiles, depending on the orientation of the rhombus. Pairs of triangles within each subset are glued together in all possible ways, where labels match, producing rhombi of the corresponding orientation.

- Triangles **A** and **B** construct diamond tiles.
- Triangles **A**, **B** and **C** construct right-sheared tiles.
- Triangles **A** and **D** construct left-sheared tiles.

The resulting tiles are almost identical to Figure 6.1, only with two extra labels on the diamond and left-sheared tiles; right-sheared tiles are the same as before. However, this new labelling scheme implies we should adjust the Column Lemma 6.3 to sum over these new labels, giving

$$\sum_{a=0}^n \text{[Diagram with label } a \text{]} = \sum_{b=0}^n \text{[Diagram with label } b \text{]}$$

where r and u are in $\{0, +\}$. The statement of Theorem 5.2 will also change, summing over all values of the extra labels along the southwest boundary and setting extra labels along the northeast boundary to 0.

References

- [1] A. Aggarwal, A. Borodin, and M. Wheeler. Colored fermionic vertex models and symmetric functions. *Communications of the American Mathematical Society*, 3:400–630, 2023.
- [2] P. Alexandersson. Non-symmetric Macdonald polynomials and Demazure–Lusztig operators. *Séminaire Lotharingien de Combinatoire*, 76:B76d, 27 pp., 2019.
- [3] S. Assaf and D. Searles. Kohnert polynomials. *Experimental Mathematics*, 31(1):93–119, 2022.
- [4] R. J. Baxter. *Exactly solved models in statistical mechanics*. Academic Press Limited, San Diego, 1982.
- [5] D. Betea and M. Wheeler. Refined Cauchy and Littlewood identities, plane partitions and symmetry classes of alternating sign matrices. *Journal of Combinatorial Theory, Series A*, 137:126–165, 2016.

- [6] D. Betea, M. Wheeler, and P. Zinn-Justin. Refined Cauchy/Littlewood identities and six-vertex model partition functions: II. proofs and new conjectures. *Journal of Algebraic Combinatorics*, 42:555–603, 2015.
- [7] A. Borodin and M. Wheeler. Nonsymmetric Macdonald polynomials via integrable vertex models. *Transactions of the American Mathematical Society*, 375:8353–8397, 2022.
- [8] B. Brubaker, V. Buciumas, D. Bump, and H. P. A. Gustafsson. Colored five-vertex models and Demazure atoms. *Journal of Combinatorial Theory*, 178:159–195, 2021.
- [9] B. Brubaker, C. Frechette, A. Hardt, E. Tibor, and K. Weber. Frozen pipes: lattice models for Grothendieck polynomials. *Algebraic Combinatorics*, 6(3):789–833, 2023.
- [10] V. Buciumas and T. Scrimshaw. Quasi-solvable lattice models for Sp_{2n} and SO_{2n+1} Demazure atoms and characters. *Forum of Mathematics, Sigma*, 10:e53, 34 pp., 2022.
- [11] V. Buciumas, T. Scrimshaw, and K. Weber. Colored five-vertex models and Lascoux polynomials and atoms. *Journal of the London Mathematical Society*, 102(3):1047–1066, 2020.
- [12] S. Corteel, A. Gitlin, D. Keating, and J. Meza. A vertex model for LLT polynomials. *Combinatorial Theory*, 2022(20):15869–15931, 2022.
- [13] M. J. Curran, C. Frechette, C. Yost-Wolff, S. W. Zhang, and V. Zhang. A lattice model for super LLT polynomials. *Combinatorial Theory*, 3(2):52 pp., 2023.
- [14] M. Demazure. Une nouvelle formule des caractères. *Bulletin des Sciences Mathématiques*, 98(3):163–172, 1974.
- [15] J. P. Ferreira. *Row-strict quasisymmetric Schur functions, characterizations of Demazure atoms, and permuted basement nonsymmetric Macdonald polynomials*. PhD thesis, University of California Davis, 2011.
- [16] A. Garbali and M. Wheeler. Modified Macdonald polynomials and integrability. *Communications in Mathematical Physics*, 374:1809–1876, 2020.
- [17] J. Haglund, K. Luoto, S. Mason, and S. van Willigenburg. Refinements of the Littlewood-Richardson rule. *Transactions of the American Mathematical Society*, 363(3):1665–1686, 2011.

- [18] A. Knutson and T. Tao. Puzzles and (equivariant) cohomology of Grassmannians. *Duke Mathematical Journal*, 119(2):221–260, 2003.
- [19] A. Knutson, T. Tao, and C. Woodward. The honeycomb model of $GL_n(\mathbb{C})$ tensor products II: puzzles determine facets of the Littlewood-Richardson cone. *Journal of the American Mathematical Society*, 17(1):19–48, 2003.
- [20] A. Knutson and P. Zinn-Justin. Schubert puzzles and integrability I: invariant trilinear forms, 2020. [arXiv:1706.10019](https://arxiv.org/abs/1706.10019).
- [21] A. Knutson and P. Zinn-Justin. Schubert puzzles and integrability II: multiplying motivic Segre classes, 2021. [arXiv:2102.00563](https://arxiv.org/abs/2102.00563).
- [22] A. Knutson and P. Zinn-Justin. Schubert puzzles and integrability III: separated descents, 2023. [arXiv:2306.13855](https://arxiv.org/abs/2306.13855).
- [23] A. Lascoux and M.-P. Schützenberger. Keys and standard bases. In *Invariant Theory and Tableaux (Minneapolis, MN, 1988)*, volume 19 of *IMA Volumes in Mathematics and its Applications*, pages 125–144. Springer, New York, 1990.
- [24] D. E. Littlewood and A. R. Richardson. Group characters and algebra. *Philosophical Transactions of the Royal Society of London. Series A, Containing Papers of a Mathematical or Physical Character*, 233:99–141, 1934.
- [25] S. Mason. A decomposition of Schur functions and an analogue of the Robinson–Schensted–Knuth algorithm. *Séminaire Lotharingien de Combinatoire*, 57:B57e, 24 pp., 2008.
- [26] T. C. Miller. Vertex models for the product of a Schur and Demazure polynomial. *Séminaire Lotharingien de Combinatoire*, 91B:100, 12 pp., 2024. FPSAC (Bochum).
- [27] K. Motegi and K. Sakai. Vertex models, TASEP and Grothendieck polynomials. *Journal of Physics A: Mathematical and Theoretical*, 46(35):355201, 26pp., 2013.
- [28] G. Orelowitz and T. Yu. Lascoux expansion of the product of a Lascoux and a stable Grothendieck, 2023. [arXiv:2312.01647](https://arxiv.org/abs/2312.01647).
- [29] A. Pun. *On decomposition of the product of Demazure atoms and Demazure characters*. PhD thesis, University of Pennsylvania, 2016.
- [30] D. Searles. Polynomial bases: positivity and Schur multiplication. *Transactions of the American Mathematical Society*, 373(2):819–847, 2020.

- [31] M. Wheeler and P. Zinn-Justin. Refined Cauchy/Littlewood identities and six-vertex model partition functions: III. deformed bosons. *Advances in Mathematics*, 299:543–600, 2016.
- [32] M. Wheeler and P. Zinn-Justin. Littlewood–Richardson coefficients for Grothendieck polynomials from integrability. *Journal für die Reine und Angewandte Mathematik*, 2019(757):159–195, 2019.
- [33] P. Zinn-Justin. Littlewood–Richardson coefficients and integrable tilings. *Electronic Journal of Combinatorics*, 16(1), 2009.